Design and Characterization of Photonic Crystal Fiber Based Surface Plasmon Resonance Refractive Index Sensor

Sayda Fahmida Kayser
Student Id: 012181007

A Thesis

in

The Department

of

Computer Science and Engineering

Presented in Partial Fulfillment of the Requirements

For the Degree of Master of Science in Computer Science and Engineering

United International University

Dhaka, Bangladesh

May 2019

Approval Certificate

This thesis titled "**Design and Characterization of Photonic Crystal Fiber Based Surface Plasmon Resonance Refractive Index Sensor**" submitted by **Sayda Fahmida Kayser**, Student ID: **012181007**, has been accepted as Satisfactory in fulfillment of the requirement for the degree of Master of Science in Computer Science and Engineering on May, 2019.

Board of Examiners

1.

________________________________ Supervisor

Md. Rabiul Hasan
Assistant Professor
Department of Electronics and Telecommunication Engineering (ETE)
Rajshahi University of Engineering & Technology (RUET)
Rajshahi-6204, Bangladesh

2.

________________________________ Co-supervisor

Dr. Raqibul Mostafa
Professor
Department of Electrical and Electronic Engineering (EEE)
United International University (UIU)
Dhaka-1212, Bangladesh

3.

________________________________ Head Examiner

Dr. Mohammad Rakibul Islam
Professor
Department of Electrical and Electronic Engineering (EEE)
Islamic University of Technology (IUT)
Gazipur-1704, Bangladesh

4.

________________________________ Ex-Officio

Dr. Mohammad Nurul Huda
Professor and MSCSE Program Director
Department of Computer Science and Engineering (CSE)
United International University (UIU)
Dhaka-1212, Bangladesh

Declaration

This is to certify that the work entitled "**Design and Characterization of Photonic Crystal Fiber Based Surface Plasmon Resonance Refractive Index Sensor**" is the outcome of the research carried out by me under the supervision of Md. Rabiul Hasan, Assistant Professor, Department of Electronics and Telecommunication Engineering (ETE), Rajshahi University of Engineering & Technology (RUET), Rajshahi-6204, Bangladesh and co-supervision of Dr. Raqibul Mostafa, Professor, Department of Electrical and Electronic Engineering (EEE), United International University (UIU), Dhaka-1212, Bangladesh.

____

Sayda Fahmida Kayser
Student ID: 012181007
MSCSE Student, Department of Computer Science and Engineering
United International University (UIU)
Dhaka-1212, Bangladesh

In my capacity as supervisor of the candidate's thesis, I certify that the above statements are true to the best of my knowledge.

____

Md. Rabiul Hasan
Assistant Professor
Department of Electronics and Telecommunication Engineering (ETE)
Rajshahi University of Engineering & Technology (RUET)
Rajshahi-6204, Bangladesh

In my capacity as co-supervisor of the candidate's thesis, I certify that the above statements are true to the best of my knowledge.

____

Dr. Raqibul Mostafa
Professor
Department of Electrical and Electronic Engineering (EEE)
United International University (UIU)
Dhaka-1212, Bangladesh

Abstract

Photonic crystal fiber (PCF) based surface plasmon resonace sensors are very popular for detecting unknown analytes. These biosensors can detect certain range of refractive indices effectively. A spiral PCF based surface plasmon resonance sensor is proposed in this paper. Gold is used as the active plasmonic material. It is placed on the external surface of the PCF. For detection purpose, the unknown analyte flow is positioned at the outer surface of the PCF. By using the finite element method (FEM), sensing performance is analyzed. The proposed sensor shows maximum amplitude sensitivity of 997 RIU^{-1} and maximum wavelength sensitivity of 10,000 nm/RIU at refractive index 1.39. At the same refractive index the sensing resolution of the sensor is 1×10^{-5} RIU. This PCF based sensor can sense the refractive indices from 1.36 to 1.39. Furthermore, performance of the sensor is investigated by varying the value of different parameters. These are gold layer thickness, pitch and air-hole diameter. The proposed sensor can detect biological analytes for its high sensitivity, improved sensing resolution and suitable linearity.

Acknowledgement

I am glad to proclaim profound gratefulness to the Allah for granting me the competency and the potency to conclude the research effectively within the preset time.

I am also pleased to convey reverence and earnest applaud to my supervisor Md. Rabiul Hasan, Assistant Professor, Department of Electronics and Telecommunication Engineering (ETE), Rajshahi University of Engineering & Technology (RUET) for his endless guidance and support during the whole research.

I am blessed to have continuous patronage from my co-supervisor Dr. Raqibul Mostafa, Professor, Department of Electrical and Electronic Engineering (EEE), United International University (UIU). I am glad to promulgate my gratefulness to Dr. Mohammad Nurul Huda, Professor and MSCSE Program Director, United International University (UIU) for his enthusiasm in my whole research.

At end, I want to applaud my parents' inspiration as well as divine love.

Table of Contents

LIST OF TABLES

LIST OF FIGURES

Chapter 1

Introduction

1.1 Background

Due to highly sensitive performance, surface plasmon resonance (SPR) is a fascinating optical detection method [1]. When light wave hits the metal field, it causes a combined oscillation of electrons at the metal-dielectric interface. This is called surface plasmon wave (SPW). A sharp incline in reflected intensity is found with the match of the energy and the momentum of the incident light and SPW. This phenomenon is called surface plasmon resonance (SPR) [2]. SPR is extremely familiar because of its extensive range of applications in environment monitoring, medical diagnostics, biological analyte detection and chemical detection over the few decades [3]. Kretschmann SPR sensors have been broadly used for its strong sensing performance but these sensors consist of moving mechanical parts and are generally bulky. Sensing applications become limited at the time of miniaturization and enhancement of these sensors. Optical fiber sensors have been introduced to get rid of these problems [4]. In recent times the main function of photonic crystal fiber (PCF) is sensing. PCF has been proven as a good replacement of prism. By harnessing its advantages such as small size, easier light launching, single mode propagation and ability in controlling evanescent field penetration, PCF turns out to be a promising candidate for SPR sensor. Small physical structure of the PCFs sensors is admirable. The sensitivity of the sensor is increased by the parameters like pitch, number of rings, air-hole dimension of the PCF [5].

SPR phenomenon is created by using gold, silver, copper and aluminium in most of the PCF based sensors at present days. As silver has no interband shift and low damping loss, it can be considered as the finest plasmonic material but when a fragile oxide layer is formed in the aqueous solution, its sensing performance is decreased [6]. Another plasmonic material aluminium, is also invaded by oxidation problem though it has high electron density. On the contrary, gold is an organic friendly metal which is also chemically stable in aqueous environment. It presents large resonance peak shift and fabrication feasibility as well [7]. PCF based sensors are generally classified in two types.

One is internal metal coated sensors. Another is external metal coated sensors. Both metal and liquid analyte are placed into discerning air hole(s) in inner section of the PCF. Plasmonic material is positioned in this section in first type. In the second type, it is accumulated on the outside layer of PCF [8]. In spite of offering high sensitivity, it is a tough job to deposit the plasmonic material accurately in labeled area of the PCF in internal metal coated sensors. In contrast, in externally metal-coated sensors plasmonic material as well as the analyte is reserved outside the PCF surface which familiarizes fabrication feasibility and high sensitivity [9].

1.2 Motivation

Biosensor is an analytical device for detecting biological and biochemical analytes by sensing their refractive index. Sensor shows different characteristics for different refractive indices. Sensitivity of a sensor designates that how much the sensor's output changes when the input quantity is measured. The main limitation of various sensors is less sensitivity. That means a shift in wavelength is extremely low. It responds to modifications in refractive index (RI) of analyte. It is viable to boost the sensor’s sensitivity. It is attained by optimizing the structural parameters of the PCF. PCF based sensors show a high wavelength shift because of minor variations in RI of analyte [2]. Besides using chemically stable materials also show large shifts in resonance wavelength. For detection accuracy sharper resonance peak is necessary [5]. Some PCF based SPR sensors offer high sensitivity as well as good detection accuracy but the design is complex for fabrication. But a simple effective design is important. A sensor is very effective which can sense wide range of RI with simple design as well as high sensitivity.

1.3 Objectives of this thesis work

In this thesis work, a spiral PCF based surface plasmon resonance (SPR) bio-sensor is proposed. The major objectives of this thesis work are:

1. Conducting an in-depth literature review related to SPR sensors.
2. Use of gold externally of the PCF structure which makes the fabrication process practical.
3. Enlarging the dynamic detection range of sample analyte.
4. Investigation of the performance of the sensor by varying performance parameter.

5. Detection of biological analytes for excellent sensitivity, better sensing resolution and appropriate linearity.

1.4 Expected outcomes

1. A novel Spiral PCF based sensor is designed for sensing unknown analytes.
2. Wide range of refractive indices can be sensed using this proposed sensor.
3. For practical fabrication gold is used externally as plasmonic material.
4. Better resolution can be achieved by the optimal design parameters which are selected carefully.
5. Enhanced sensitivity can be attained which is ensured by efficient investigation of design parameters of the proposed sensor.
6. A SPR sensor with linear characteristic is presented in this work.

1.5 Methodology

In this chapter, all numerical tools employed in the realization of the bio sensor are included. Methods used in this work are also introduced here. These methods as well as the numerical tools are useful to obtain the objective.

1.5.1 Finite Element Method

Finite Element method (FEM) is a mathematical procedure to find out probable solutions of boundary value problems for partial differential equations. Finite elements are the subsection of an entire problem domain into ordinary portion. The variational methods were applied to solve the problem by reducing an affiliated error function. A complicated equation is inferred over a greater domain. It is accomplished by adjoining multiple simple element equations over many short subdomains. These elements are designated as finite elements in FEM [55]. As this discrete element model was a variant process to solve the continuum mechanics problems, the term finite element method was constructed.

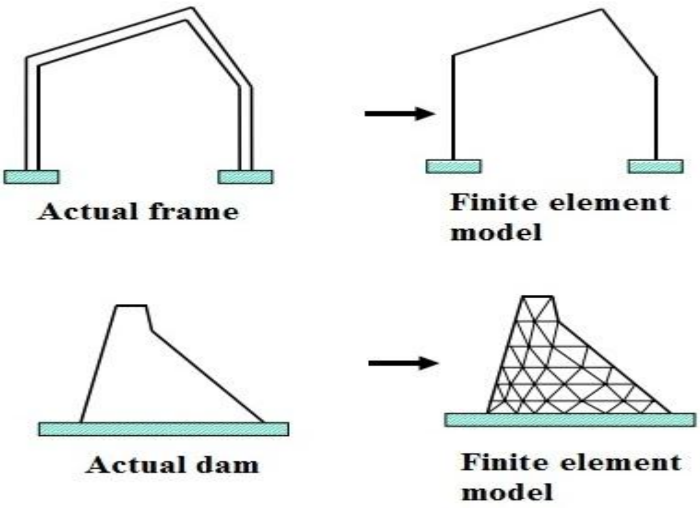

Figure 1: The Finite Element Idealization [56]

Figure 5. exhibits that models for both consecutive structures and frame structures were formed as a system of elements interlinked at joints or nodes. In many studies on structural analysis, it has comprehended the potency to solve problems in continuum mechanics by applying discrete elements.

1.5.2 Perfectly Matched Layer (PML)

Perfectly matched layer, a kind of absorbing layer, is applied to model the radiation damping using FEM. It makes the dynamic analysis more accurate. The PML is able to absorb incident waves under any angle and frequency that ensures them to pass through the model boundaries without reflection [57]. This absorbing material must have matching anisotropic permeability and permittivity with the physical medium outside the PML. To express the PML, Maxwell’s equations can be used. By introducing a complex valued coordinate, the wave impedance remains unaffected [57].

1.5.3 Numerical Modeling and Sensor Design

1.5.3.1 Effective Refractive Index

To calculate the phase change per unit length in identical transparent media, refractive index n can be applied. The phase variation is n times larger than in vacuum. The effective refractive index n_{eff} has the uniform meaning for light propagation in waveguide. It relies on wavelength and light propagation mode. Imaginary part can define gain or loss as the effective index may be a complicated portion [58].

1.5.3.2 Confinement Loss

Confinement loss is a measurable factor utilized in optical fiber for representing its light confinement capability in core region. In PCF if the number of air-hole rings is increased, light confines at core region appreciably. Hence confinement loss is reduced. Fortunately, we can retain the confinement loss within a preferred value since there is a design independency in PCF to select compatible number of air-hole rings [59]. Those which hold more air holes rings have less losses. This loss Lc is acquired as -

$$L_c(\text{dB/cm}) = 8.686 \times k_0 \,\text{Im}[n_{eff}] \times 10^4 \qquad [1.1]$$

Where Im [η_{eff}] is the imaginary part, $k_0 = 2\pi/\lambda$. Using Maxwell's equations as an eigen value problem with the FEM, the complex RI of fundamental mode can be solved [60]. This loss depends on many factors. Core size is one of these factors. Pitch and air-hole dimension are another factors. Number of rings in the cladding is also significant. We have opportunity to get suitable fiber with very low loss for PCF.

1.5.3.3 Wavelength Interrogation Method

The Maximum resonance wavelength shift has many functions. For example, Sensitivity of a sensor depends on it. It can be computed using wavelength interrogation method. This method has many advantages over Amplitude detection method. It provides higher sensitivity and detection range. Sensitivity here is defined as [28]

$$S_\lambda(\text{nm/RIU}) = \Delta\lambda_{peak} / \Delta n_a \qquad [1.2]$$

Where λpeak represents the peak wavelength shift for any variation in analyte RI. Δna is the difference between two consecutive RIs.

1.5.3.4 Amplitude Interrogation method

Amplitude sensitivity does not require wavelength interpolation and so it is simple and economic. Sensitivity here is expressed as [48].

$$S_A(\text{RIU}^{-1}) = -\frac{1}{\alpha(\lambda, n_a)} \frac{\partial \alpha(\lambda, n_a)}{\partial n_a} \qquad [1.3]$$

Here, n_a is analyte RI and for this, $\alpha(\lambda, n_a)$ is the confinement loss. Again confinement loss difference is prescribed as $\delta\alpha(\lambda, n_a)$.

1.5.4 Numerical Tools

There are three numerical tools used in this thesis. They are as follow:

One of the most powerful softwares is the Comsol Multiphysics. It can accomplish eigen-frequency and modal analysis. The software employs the proven finite element method (FEM). It runs finite element analysis with adaptive meshing. It can also control errors with many numerical solvers. With this you can design Photonic crystal fibers easily by defining the sub-domains and boundary conditions with correct parameters and also you can solve the problems for both electric field and magnetic field. For designing the structure Comsol Multiphysics version 4.2 is used. Secondly, MATLAB software is used in this thesis to assess the performance of the sensor, confinement loss and sensitivity curve. Thirdly, Microsoft Excel is also used to preserve the data collected from Comsol software which are processed in MATLAB later for getting the desired curves.

1.6 Thesis organization

The thesis comprises six chapters. These illustrate the extensive work to attain the objectives which are described earlier.

Chapter 1 discusses background of PCF based SPR biosensors and objectives of this thesis. Describes detail methods used in this work. It further narrates the whole work.

Chapter 2 concentrates on the literature review of the prevailing work on PCF SPR sensors. It also states the outcome of the work.

Chapter 3 explains the working principle of PCF and SPR. The application of SPR sensor is also included in this chapter.

Chapter 4 describes the structure of the proposed PCF based SPR sensor. The performance parameters are studied and results are also discussed in this chapter.

Chapter 5 concludes the whole work. Suggestions for future work are also included there.

1.7 Summary

The conciseness of the research has been provided in this chapter. In addition, the goals and purposes of the research have been stated which give an obvious idea on the whole research.

Chapter 2

Background and Literature Review

2.1 Background

The comprehensible facts of SPR were first explained by Wood in 1902 [10, 2]. He noticed a shape of "exceptional" divergent in the mirrored light. When the polarized light blazed on looking glass with a scattering grating. Thereafter, in lieu of trying to describe this fascinating phenomenon for decades, an extensive interpretation of SPR could not be offered until 1968. The incitement of the surface plasmons is caused through attenuated total reflection (ATR) technique on the basis of an analogous prism coupling formation correspondingly according to the announcement from Otto [11], Kretschmann and Raether [2] in 1968. The expected usage of SPR for sensing motives began in late seventies [12, 13].

In 1983, Liedberg et al firstly exhibited the usance of SPR based sensor to monitor the biomolecular interaction [14]. They were skilled to comprehend the straight and instantaneous detection of the bio-molecular interaction by applying the SPR sensing method. SPR sensing technology has been acquiring a massive interest as well as improving constantly from then. On the basis of Kretschmann configuration named the Biacore instrument, the first commercial SPR biosensor commenced in 1990. More firms devoted themselves for improving the marketable SPR instruments having distinct characteristics after the triumph of Biacore SPR. Great efforts have been given till now for the advancement of modern SPR based devices as well as for alternation of the SPR sensor for different objectives, particularly for instantaneous bio-sensing. SPR technology has been contributing significantly in the areas of chemical and biological studies as a leading sensing technology.

In 1966 optical fibers developed arenas such as and sensing and telecommunications. Using its light guidance high sensitivity achieved. It became remarkable for its geometric changeability and enlarged sensitivity over remaining procedures. Optical fibers based sensors are better solution for many industries for their strength, mobility, tremendous sensitivity [9]. Moreover, they have usability in intense electromagnetic field, noise, high voltages, nuclear radiation etc. The arrival of photonic crystal fibers (PCFs) in 1996 was a revolution in fiber optic technology. many limitations of conventional fibers are overcome by them [11]. PCF is a single material fiber. It has array of air holes in its cladding. The utmost attraction in PCF is, it is possible to achieve the desired value by changing the structural parameters. Preferred sensitivity, nonlinearity, dispersion, birefringence can be attained. Refractive index is a basic material property. Its exact measuring is vital in many applications. PCF based refractive index sensors are attractive, for their small size, flexibility in their design.

2.2 Literature Review

In PCF based SPR sensors different kinds of plasmonic materials are used such as gold, copper, silver, and aluminum plasmonic materials [15]. These plasmonic materials can be put externally or internally. Many previous works of different design with different plasmonic material are studied. Internally coated PCF is reported in [16]. A thin gold and TiO_2 film are placed on air holes' surface. In [17] a hollow core photonic crystal fiber (HC-PCF) is planned. The analyte and silver nanowires are positioned in HC-PCF's air holes and paper [18] presented microfluidic slots. In [19] metal layer is deposited within the PCF. Liquid analytes are selectively occupied within the inner air hole(s). Now-a-days, indium tin oxide (ITO)-based SPR sensors have gained more attraction for small volume plasma frequency [19]. A PCF with liquid core and two selectively analyte-filled channels is proposed in [20], where graphene–silver coating enhances the sensing performance. In [21] Fan et al. demonstrated a PCF SPR sensor particularly filled with analyte which exhibits wavelength sensitivity 7040 nm/RIU using gold as plasmonic material. It is 7017 nm/RIU for silver. A PCF using graphene–silver bimetallic configuration exhibited wavelength sensitivity of 2520 nm/RIU. It also shows amplitude sensitivity of 72.47 RIU^{-1} [17]. Practically, it is tough to fill the air holes with analyte particularly. A hollow-core PCF sensor including open ring channel is introduced to overcome this limitation that functions in the mid-infrared region [22].

PCF SPR sensor with bigger microfluidic channels is proposed in [23]. This PCF shows wavelength sensitivity of 2000 nm/RIU. It appears amplitude sensitivity of 300 RIU^{-1} at refractive indices from 1.33 to 1.39 [23]. The existing paper [24] offered a grapheme based PCF with high sensitivity which is birefringent in nature but it includes four different diameter's air holes. Another grapheme based PCF of D-Shaped is exhibited wavelength sensitivity 3700 nm/RIU. It displayed resolution of 2.7×10^{-5} RIU in [2]. A D-Shaped PCF modeled in [5]. It provided average and maximum sensitivity 7700 and 9000 nm/RIU respectively. Though D-Shaped PCFs help to overcome the problem of internal coating, for attaining flat surface they need extra surface polishing which makes complications in manufacturing [25]. In [26] a SPR-PCF with dual coating of gold and Tantalum pentoxide layer is used which provides high sensitivity of 9180 nm/RIU with resolution 1.09×10^{-5} RIU at near infrared wavelength. In recent time, SPR sensor constructed with a diamond ring fiber (DRF) has been advised with numerical investigations in [27]. An externally dual coated (gold and Tantalum pentoxide layer) multi-core flat fiber (MCFF) based SPR is presented in [28] to identify analyte of high refractive index from 1.46 to 1.48. It shows maximum sensitivity 23,000 nm/RIU. It demonstrates RI resolution 4.35×10^{-6}. Two externally gold coated hexagonal photonic crystal fibers (H-PCFs) are investigated in [29] also in [30]. The paper [29] exhibits wavelength sensitivity 4000 nm/RIU and amplitude sensitivity 478 RIU^{-1}. These are realized with resolution 2.5×10^{-5} and 2.1×10^{-5} RIU respectively at refractive indices range of 1.33-1.37. In [30], wavelength sensitivity 4000 nm/RIU with amplitude sensitivity 320 RIU^{-1} are attained with the sensor resolutions 2.5×10^{-5} and 3.125×10^{-5} RIU at sensing range 1.34 to 1.36. Besides, [31] modeled an H-PCF with an ultrathin niobium nanofilm as plasmonic material. Al_2O_3 film is put on outside surface of niobium film for increasing the coupling strength. It presents wavelength sensitivity 8000 nm/RIU. It also offers maximum amplitude sensitivity 1560 RIU^{-1} for an analyte index 1.40.

In [32] a PCF SPR sensor with elliptical air holes and four microfluidic channels is offered that can sense multiple analytes. A multi-channel PCF-based sensor using plasmonic material silver which is coated with the gold has been presented in [33]. It demonstrates wavelength and amplitude sensitivity 4750 nm/RIU 1555 RIU^{-1}[33]. A D-shaped hollow-core PCF sensor shows wavelength and amplitude sensitivity 6000 nm/RIU and 148 RIU^{-1} [34]. ITO is used as the plasmonic material. Another hollow-core PCF SPR sensor presents maximum wavelength sensitivity 4000 nm/RIU with amplitude sensitivity 478 RIU^{-1} [9]. In [35] a copper–graphene-based PCF sensor is proposed. It illustrates wavelength sensitivity 2000 nm/RIU, also amplitude sensitivity 140 RIU^{-1}. The sensing range is 1.33 to 1.37. A hexagonal PCF sensor is exhibited in [36]. It combines single ring and four microfluidic channels, for multi-analyte detections four modes are separately studied there. This sensor indicates wavelength sensitivity 2400 nm/RIU in range 1.33 and 1.34.

To date, numerous PCF SPR sensors have been reported. From the above study, various kinds of sensors of different wavelength and amplitude sensitivity are observed. All have diverse structures. Problems statements are some sensors have low sensitivity and some offered difficult designs. High sensitivity and fine resolution is desirable for a good sensor. On the other hand the scope of practical fabrication is essential for a design. Some proposed design put plasmonic material in internal air holes which is tough for fabrication. Previous study showed the scope for spiral fabrication as well as external covering surface with material. Low linearity is also deficient for a sensor. It is the scale of measurement for the correctness of detection procedure. Proposed sensor of this work focused on all of these issues.

This paper explores a simple spiral PCF to gain high sensitivity. A layer of gold is used as plasmonic material in the outer surface of the PCF structure. It is done to simplify detection mechanism and fabrication process. There are many performance parameters of sensor. Wavelength sensitivity, amplitude sensitivity, sensor resolution and linearity are mainly used. These are numerically investigated at analyte refractive index between 1.36 and 1.39. To acquire the optimal sensing performance, design parameters are studied here. These include pitch, air hole diameter and gold layer thickness.

Chapter 3

Photonic Crystal Fiber and Surface Plasmon Resonance

3.1 Photonic Crystal Fiber (PCF)

3.1.1 History of PCF

Optical fiber is a cylindrical waveguide. In the middle, solid glass core runs down with high refractive index, other portion has the lower. It borders the core and makes homogenous cladding [37]. Index difference between the core and cladding facilitates to trap light inside core. Through total internal reflection mechanism, light is guided along the length of fiber. This category of fiber is called conventional optical fiber. On the basis of the features of photonic crystals, PCF is a new category. Its capacity to confine light in hollow cores or obstruction natures is not probable in traditional fiber [38]. PCFs or holey fibers or microstructure optical fibers contain microscopic air channels. These channels establish a less index cladding around undoped silica core [39]. In present days, PCF is searching its usages in fibre-optic area, highly sensitive sensors, nonlinear devices, high-power transmission and so on. Various parameters can be regulated in PCF. These are air hole shape and diameter, RI of glass, nature of lattice, distance between hole to hole known as lattice pitch.

Yeh et al. gave the concept of a PCF for the first time in 1978 [40]. Cladding a fiber core using Bragg grating was offered by him. This is analogous to 1D photonic crystal. P. Russell invented a PCF containing 2D photonic crystal with air core in 1992. The first PCF was revealed at Optical Fiber Conference (OFC) in 1996. In 2000, eminently birefringent PCF was offered and supercontinuum construction having PCF was familiarized for the first time [40]. Formation of a Bragg fiber was made firstly in 2001. In that year, PCF laser with twofold cladding was delivered as well for the first time [39]. In the year 2002, PCF with ultra-flattened dispersion was commenced. Large power transmission, Low-loss alterations among PCFs and Photonic band gaps at 1% index contrast were promoted in 2005. Polarization reliance of stimulated Brillouin spattering in small-core PCFs was founded firstly in 2008. Nonlinear inter-core coupling in triple-core PCFs was introduced afterwards in 2009 [41]. Then in the year 2010, Diffraction and nonlinear coefficients of PCF were founded on the basis of degenerating four wave mixtures. An elliptical type of honeycomb porous-core PC-PBGF was offered for the first time in 2011.

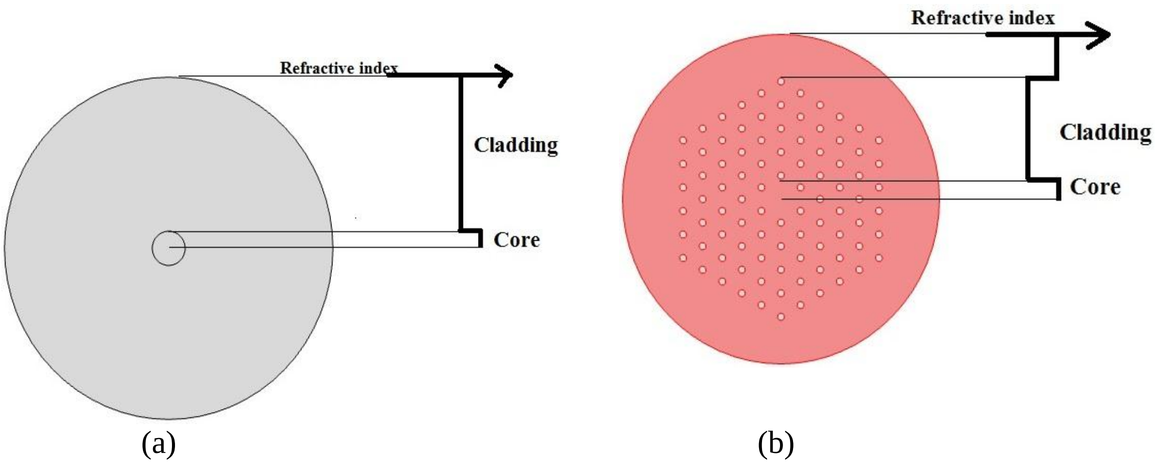

Figure 2: (a) Conventional step-index fiber (b) Photonic crystal fiber

Figure 1. (a) depicts a SI fiber with superior index doped core. Light is restricted to the core by TIR at core cladding interfaces. Figure 1. (b) delineates a PCF. It is constructed from a single material. This material has many air holes in the cladding.

3.1.2 Light Guiding Mechanism of PCF

Total Internal Reflection (TIR) is the most basic and well known principle of guiding light in traditional fibers. The most of the TIR crystal fibers have solid core enclosed by a covering with a regular periodic array of air holes. These holes form effective refractive index of covering region lower than pure silica, so light trapped in the solid core area, which has a relatively higher RI [42]. A graphical representation of cross section of such PCF is given below in Figure 2. which portrays the propagation of light with TIR.

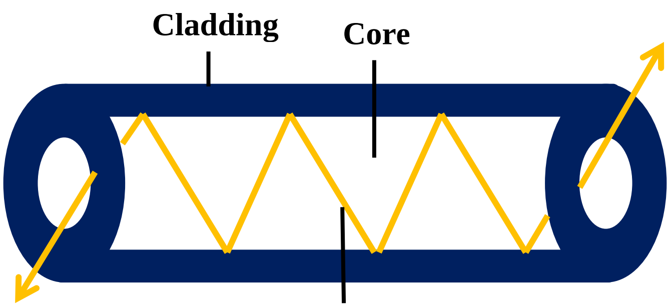

Figure 3: A fiber passing light with TIR

The refractive index of the microstructured cladding in PCFs depicts a wavelength dependency. This strong dependence permits design of numerous single-moded fibers. But only a single mode is supported irrespective of optical wavelength. Fibers with highly large mode field diameters are prepared, probable for specific control of the refractive index profile [43].

The PCF absorbed the photonic band gap (PBG) effect to guide light. It was testified first in 1998. PBG fibers cannot be constructed from traditional optics. These are associated to Bragg fibers, as they are not dependable on TIR for guiding light. Ordinary optic fibers cannot constitute hollow cores fibers because guidance by TIR needs a lower-index cladding material to be used for adjoining the core. The only compatible low-loss materials including lower RI is air at optical frequencies. An extra hole is introduced to the solid core for lowering the effective index of the core [44]. Hollow core guidance becomes possible in PBG guidance. If periodicity of the structure is cracked by a fault, a specific area having optical features varied from the photonic crystal is generated. The defect region can boost the modes along frequencies fallen within photonic band gap, which obstruct them from diffraction of photonic crystal. PBG is accountable for confining the light in core. So it’s not mandatory that the defect region has larger refractive index than the surrounding [45].

Limiting losses in hollow-core fibers follow the similar techniques that restrict loss in traditional fibers. Losses in existing fibers involve absorption, Rayleigh scattering, confinement loss, bend loss including alterations in the fiber formation. These may be diminished within the limits observed in traditional fibers since the larger portion of light moves in hollow core, where dispersion as well as exploitation could be extremely less

[46]. PBGs appear fascinating but TIR PCFs also exhibit identical characteristics, in this subsequent discussion of this research, the PCF directs to silica TIR PCF unless PBG.

3.2 Surface Plasmon Resonance sensor

3.2.1 SPR Basis

Surface plasmon (SP) is the movement of many electrons at metal-dielectric interface. Surface plasmon resonance (SPR) is the propagation of surface plasmon wave (SPW) along this interface [47]. It occurs if the light photons' frequency equivalents the usual frequency of surface electrons. The electrons oscillation is induced by the incident light. SPW is an electromagnetic wave obtained from solving Maxwell's equation. The field force of SPW is highest at the metal-dielectric interaction. It reduces significantly into both metal as well as dielectric media as depicted in Figure 3.

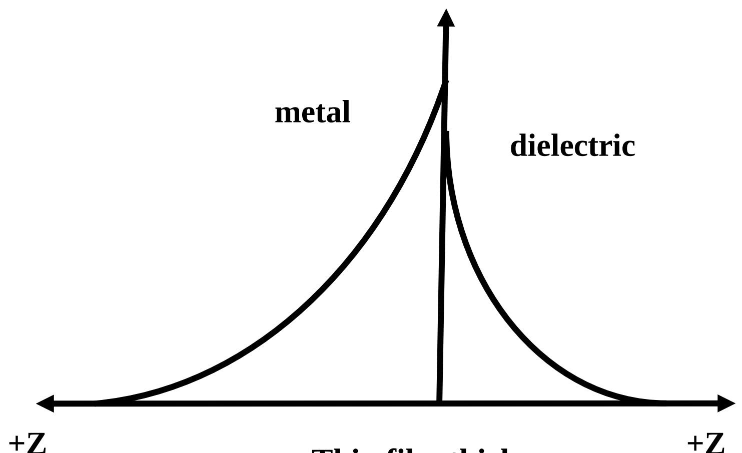

Figure 4: Variation of field intensity with respect to film thickness [48].

SPW propagates towards metal-dielectric interface. It circulates with propagation constant (k_{sp}) as per Maxwell's theory. The expression of it [49]:

$$k_{sp} = \frac{\omega}{c}\sqrt{\frac{\varepsilon_m \varepsilon_d}{\varepsilon_m + \varepsilon_d}} \qquad [3.1]$$

Where ε_m signifies dielectric constant of metal layer. Again ε_d stands for the dielectric medium. In accordance with the equation 3.1, the SPW characteristics are exceedingly reliant on metal media. These count on dielectric medium too. When light propagates throughout the dielectric medium, the propagation constant of light k_D specifies as [49]:

$$k_D = \frac{\omega}{c}\sqrt{\varepsilon_d} \qquad [3.2]$$

Where ε_d is the dielectric constant. As portrayed in Figure 4, the dispersion relation of SPW never intersects light roaming in dielectric medium ε_d (for example, in air). It depicts that at metal-dielectric interface, incident light cannot directly stimulate the SPR. Therefore, the energy of incidental light in dielectric medium needed to increase for being similar with SPW to excite SPR.

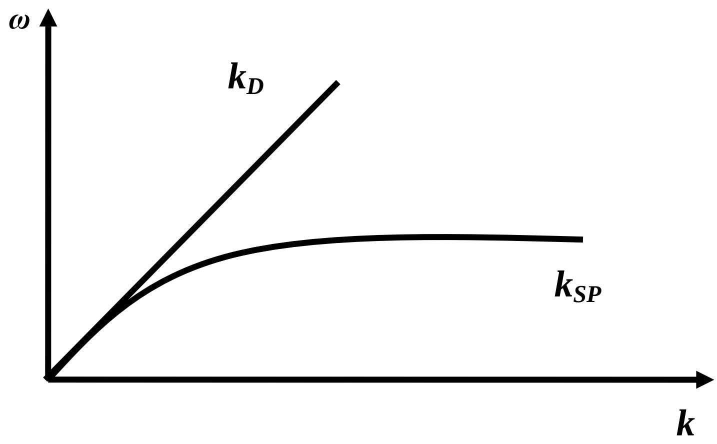

Figure 5: Relation between SPW (k_{SP}) and light in dielectric medium (k_D). [48].

3.2.2 Excitation of SPR

3.2.2.1 Otto configuration

In 1968, Otto configuration was published. It is an ATR procedure for exciting SPR. It is performed through coupling evanescent wave (EW) and SPW. It is the idea behind this configuration. It is done at metal-dielectric interface by prism reliant design. The EW is an electromagnetic wave with intensity declining remarkably in the media. Remaining an air gap between prism base and metal coating, the metal surface is placed nearness to evanescent field. However, in practical, this design is tough to materialize because the metal should be positioned within approximately 200 nm of the prism surface [50].

3.2.2.2 Kretschmann Configuration

In the same year, a prism based SPR configuration was stated by Kretschmann and Raether, which is known as Kretschmann configuration. They observed the connection of the metal layer with the prism base. For this, EW might be produced at the prism-metal interaction. Again thickness of the metal becomes small enough. So at metal-dielectric interface, EW could also excite SPR [51]. There are many ways to overcome the limitations of Otto configuration. One way is to coating a very thin metal film approximately 50 nm kept in direct vicinity with the dielectric medium having less refractive index.

EW is produced at prism-metal interface. To generate it, the incident angle of polarized light becomes coequal or larger than the critical angle. Then it enters into the metal and couples with SPW. After that it stimulates the SPR. There are drawbacks of Otto configuration. One of the solutions is that the target analytes are in contact with the metal surface [51].

3.2.3 Sensing principle

Basically SPR sensor finds variation of RI in sensing area. The incident light attaches with the surface plasmon waves. So some energy is shifted into the free electrons. Then these electrons begin to vacillate at metal dielectric interface. The condition for SPR excitation will change with a small changing in refractive index. The change in RI is caused by the bio-molecular interface.

The energy shifted from the incident light is varied by RI alteration. Consequently, the coupling situation between a light wave and surface plasmon is altered. The modification in optical properties of the reflected light is observed. So change in refractive index around the sensing surface can be identified [52].

3.2.4 Optical fiber based SPR sensor

In early nineties the development of fiber-optic SPR sensors began [48]. Based on total internal reflection (TIR) in optical fiber, guidance of light occurs which leads for the incitation of SPR. Light traveling along an optical fiber contains two components. One is the TIR guided field in fiber core. Another is significantly declining evanescent field originated at core cladding interaction. The prism is applied to attain TIR and EW for exciting SPR in prism based SPR sensor. Optical fiber can also be conducted for the similar reason. The optical fiber based SPR sensors have more benefits over the general prism based SPR sensors. Small sample prerequisite is one of these. They provide simplified and malleable sensor design. Abridged sensor system is another advantage. The other benefits include remote sensing capacity and obstacle to electromagnetic intervention. Fiber-optic based SPR sensors become interesting as well as promising for their mechanical flexibility [48].

3.2.5 Photonic crystal fiber based SPR sensor

The cladding area of PCFs has periodic air holes unlike the conventional optical fiber which manages the light propagation. The PCFs follow customized TIR or PBG effects for the propagation of light. Light propagation can be regulated mainly in two ways. One is to vary air holes geometries. Another is to alter the number of rings. These skills of PCF overcome the problems of traditional prism and optical fiber based SPR sensors [3]. The advantage of PCF SPR sensors is their compactness and flexibility in design. In PCF, core-cladding diameter and location can be optimized. So the light in single mode is attained. Single mode PCFs exhibit narrow-band resonance peak. So sensitivity is increased. In PCF based SPR sensors, the constructive elements of the machine are optimized. As a result, the sensing range and sensitivity can be improved [53].

3.2.6 Application of SPR based sensor

Due to several promising applications, surface plasmon resonance (SPR) has drawn more attraction. It has a huge impact on biosensing, chemical detection and environmental monitoring. SPR plays significant role on bioimaging, liquid detection, gas detection, medical diagnostics also. Successful applications of optoelectronic devices such as optical tunable filters have become possible for wide-range research on SPR technology. The application also includes thin-film thickness monitoring [54].

3.3 Summary

In this section, the background of PCF and SPR are studied. Previous work and the development of SPR have been analyzed. The sensing theory and features of PCF based SPR has also been introduced and explained. Applications of SPR have been reviewed here.

Chapter 4

Proposed Structural Design and Simulation

4.1 Introduction

The design of PCF can be different like hexagonal, octagonal, spiral, D shaped for various purposes. For obtaining the desired result an optimal design is found out. In this work spiral PCF is proposed. COMSOL 4.2 software is used here for the design and simulation purpose. Using the FEM, guiding estates of the PCF are evaluated. PML boundary condition is used. In this chapter, proposed design is explained elaborately. PCF based sensor's sensing properties are also explored here by varying PCF parameters. All the results are discussed in details in this chapter.

4.2 Sensor design

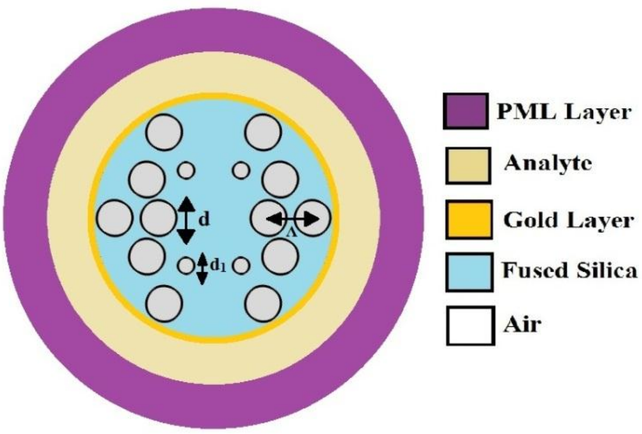

Figure 6: Cross section view of the proposed sensor.

Figure 6. displays the cross segment view of the spiral PCF containing three rings. In the same ring it reserved 60 degree angle among two air holes. Identical spiral arm's air holes have consecutive angular shift (θ) of 30 degree. Distance from the center of one hole to other is entitled as pitch, Λ which is 2 μm here. The second and the third ring are located at 1.4 × Λ and 1.8 × Λ distances respectively from the central air hole. Inside the fourth ring, four smaller air holes' diameter is $d_1 = 0.3 \times \Lambda$. For the rest air holes, $d = 0.65 \times \Lambda$

is the diameter. Two vertical air holes of the second ring and central air hole are eliminated so that contact of transitory field with the sensing layer is increased. Structure of the proposed design is constructed with fused silica and all the air holes are empty. Outer surface is 40 nm gold layer coated (t_g). Using Drude- Lorentz model, the permittivity of gold material can be obtained [4].

$$\varepsilon_{Au} = \varepsilon_{\infty} - \frac{\omega_D^2}{\omega(\omega + j\gamma_D)} - \frac{\Delta\varepsilon\Omega_L^2}{(\omega^2 - \Omega_L^2) + j\Gamma_L\omega} \quad [4.1]$$

The associated values of the constants are taken from [9]. As the sensing medium, analyte layer is placed above the gold layer. PML is the outmost layer. PML and analyte layer's width are 2 µm and 1.8 µm individually. After the convergence test analyte layer's depth is established which improves the simulation results and accuracy. The thickness of analyte layer was varied from 0.25 µm to 15 µm. The increment in analyte layer thickness after 1.5 µm causes very small variation in the effective index's imaginary part. Contrariwise, more thickness of the analyte layer increases simulation time. So to keep up a stability between simulation speed and simulation results exactness of the, 1.8 µm is used as the optimal analyte layer thickness.

When electromagnetic wave hits the metal field, a joint fluctuation of electrons at the metal dielectric boundary is occurred which is called surface plasmon wave. Core guided mode as well as surface plasmon polariton (SPP) mode has an important contribution to know unknown analyte's RI. Figure 7. (a), (b) represent x-polarized core mode and SPP mode respectively at analyte RI 1.36, functional wavelength of 0.69 µm.

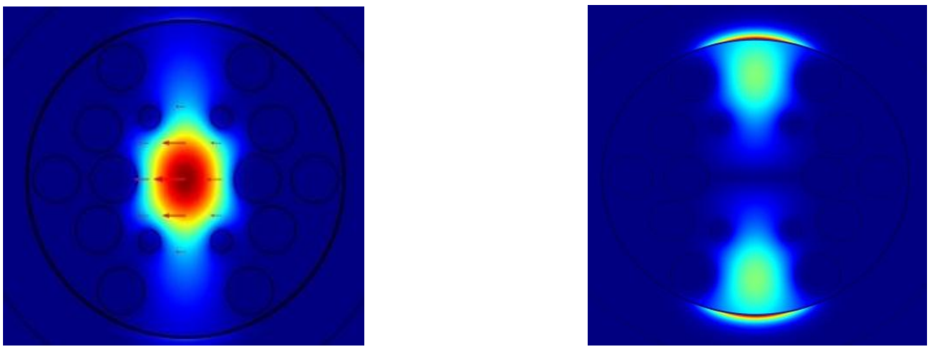

Figure 7: Fundamental x-polarized (a) core mode, (b) SPP mode.

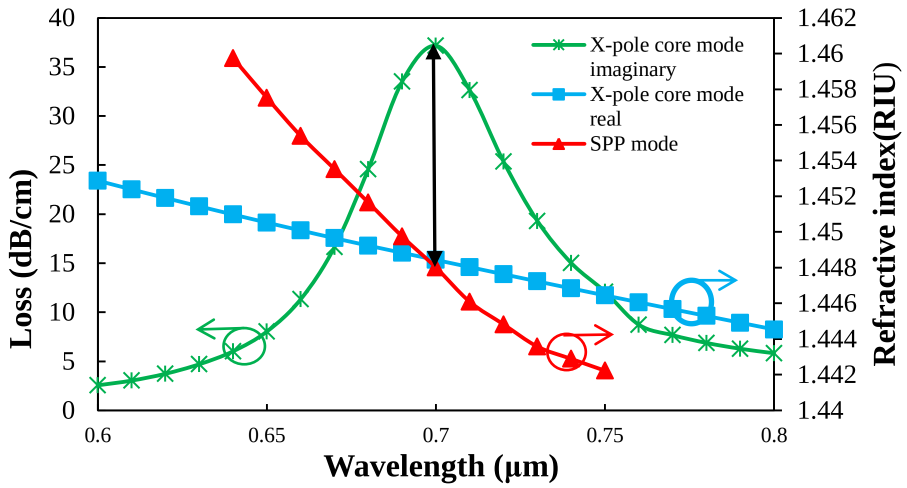

Figure 8: Relation between SPP mode and x-polarized core guided mode.

In Fig. 8, the resonant frequency range and basic two modes (core guided, SPP) are shown at n_a= 1.36 in x-polarization. Dispersion relationship studied considering plasmonic material gold, where t_g=40 nm. With the blue and red line, real parts of the n_{eff}, of fundamental mode and SPP mode are donated respectively. At 0.69 µm (resonated wavelength), the effective index of the fundamental mode (blue) and SPP mode (red) matched where a loss peak is found.

4.3 Sensor Performance and Optimization

4.3.1 Wavelength sensitivity and resolution

Confinement loss is an important aspect. To determine the loss, imaginary part of the refractive index (n_{eff}) is used; its equation is taken from [17].

$$L_c(\text{dB/cm}) = 8.686 \times k_0 \,\text{Im}[n_{eff}] \times 10^4 \quad [4.2]$$

Where $I_m[n_{eff}]$ is refractive index's imaginary part with unit dB/cm.

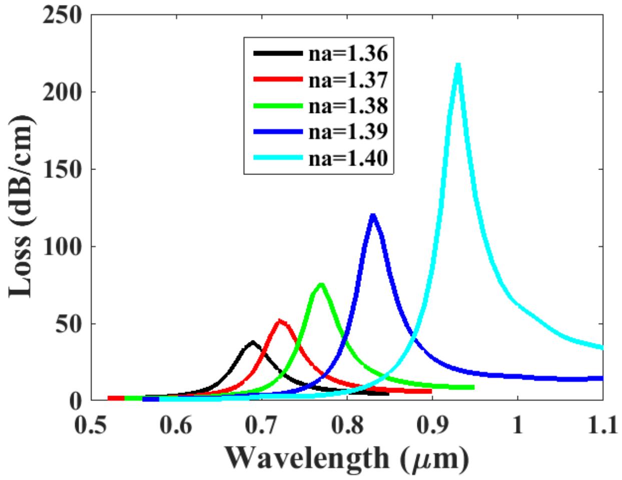

Figure 9: Loss spectrum with RI variation for optimum design.

Figure 9. shows the confinement loss deviation with the alteration of refractive indices for 2 μm pitch, 0.3 and 0.65 μm air hole diameters and 40 nm gold coating. The consistent loss is 37.7 dB/cm at RI 1.36 in the wavelength 690 nm. It is observed that when the analyte RI is increased from 1.36 to 1.40 (having step size 0.01), the peak loss depth is also increased. The substantial change of confinement loss occurs as analyte RI incremented. When analyte RI rises the index difference among core and SPP mode turns to be lesser. Furthermore, increase in the analyte RI (a red shift is noticed) alters the point of identical phase to upper wavelengths. Loss depths are 51.5, 76, 121 and 218 dB/cm orderly at refractive indices 1.37, 1.38, 1.39 and1.40 in the wavelengths 720, 770, 830 and 930 nm respectively. Enhanced confinement is directed by the high loss depth that increases the intrusion of field across the cladding section. For this, advanced energy shifts from core mode to the SPP mode and interaction with analyte enhances. The resonance wavelength shifts are 30, 50, 60, 100 with analyte RI varied from 1.36 to 1.37, 1.37 to 1.38, 1.38 to 1.39, 1.39 to 1.40 individually.

Resonance wavelength move causes sensitivity that can be computed by using wavelength interrogation method. From [24] the equation of wavelength sensitivity is taken.

$$S_{\lambda}(\text{nm/RIU}) = \Delta\lambda_{peak} / \Delta n_a \quad [4.3]$$

Where λ_{peak} means peak wavelength shift for analyte RI variation, Δn_a is the difference between two sequential analyte RI. The theoretical wavelength sensitivities are obtained as 3000, 5000, 6000, 10000 nm/RIU at 1.36, 1.37, 1.38 and 1.39 respectively. Another important parameter is sensor resolution. It can be achieved by using wavelength interrogation method. We used the equation of sensor resolution from [17].

$$R(RIU) = \Delta n_a \times \Delta\lambda_{min} / \Delta\lambda_{peak} \qquad [4.4]$$

In equation (3), λ_{min} denotes lowest spectral resolution. Wavelength resolutions are 3.33×10^{-5}, 2×10^{-5}, 1.67×10^{-5} and 1×10^{-5} RIU at 1.36, 1.37, 1.38 and 1.39 orderly.

4.3.2 Amplitude sensitivity and resolution

The implementation of wavelength interrogation method is expensive as it provides sensitivity at specific wavelength only. But amplitude sensitivity does not require wavelength interpolation and so it is simple and economic. The equation of amplitude sensitivity is taken from [48].

$$S_A(RIU^{-1}) = -\frac{1}{\alpha(\lambda, n_a)} \frac{\partial\alpha(\lambda, n_a)}{\partial n_a} \qquad [4.5]$$

In 5.5, n_a signifies analyte refractive index and for this, $\alpha(\lambda, n_a)$ is the confinement loss. Again $\delta\alpha(\lambda, n_a)$ is the confinement loss difference for two adjacent analyte RIs.

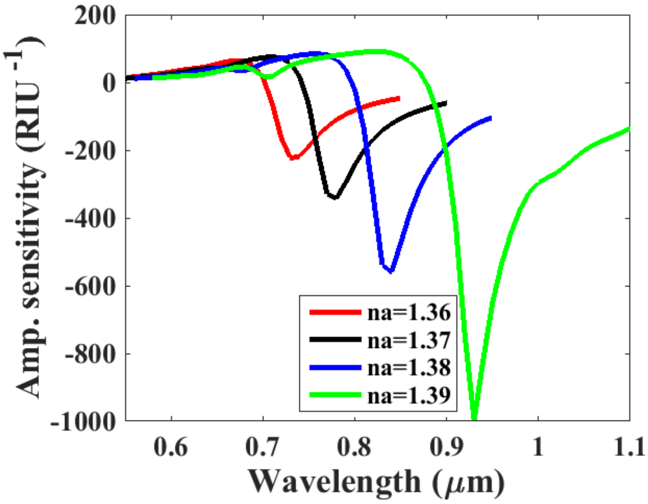

Figure 10: Amplitude sensitivity with RI variation for optimum design.

Figure 10. depicts amplitude sensitivity of 224, 343, 560, 997 RIU^{-1} respectively for 1.36, 1.37, 1.38 and 1.39 RIs and optimal parameters. Amplitude sensor resolutions attained using amplitude interrogation method are 4.46×10^{-5}, 2.92×10^{-5}, 1.79×10^{-5} and 1×10^{-5} RIU.

4.3.3 Gold thickness variation

Alteration of gold layer width has visible impact on loss depth and amplitude sensitivity.

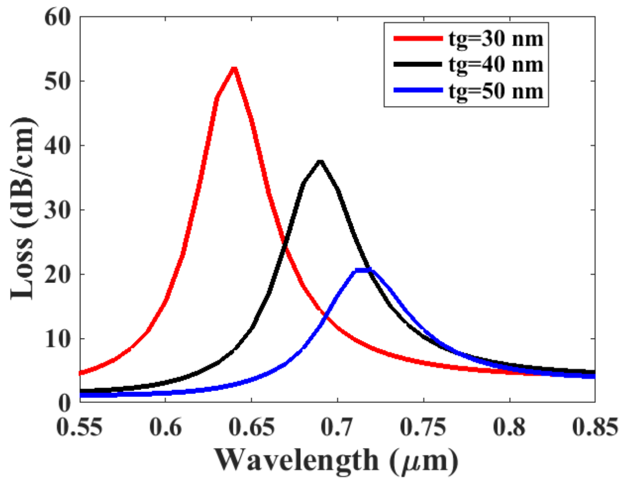

Figure 11: Loss spectrum with gold layer thickness variation.

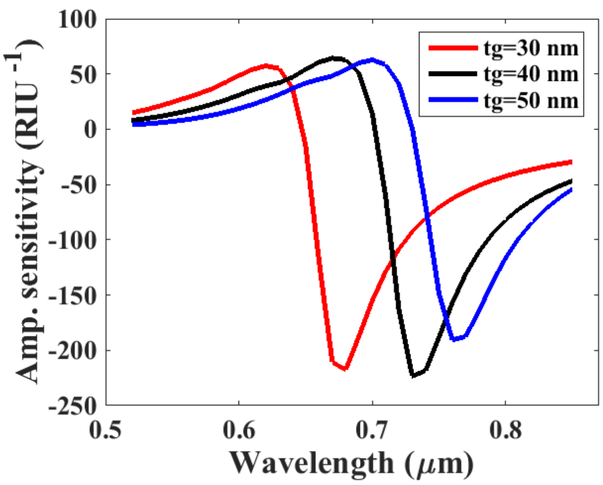

Figure 12: Amplitude sensitivity with gold layer thickness variation.

Figure 11. shows that at RI 1.36, the confinement losses are 52, 37.7 and 20.5 dB/cm when the depth of gold layer is correspondingly 30, 40 and 50 nm. So, loss is declined with the rise of t_g. Blue shift occurs in the loss curve for alternation of gold coat's width. Besides, Figure 12. illustrates that at RI 1.36, amplitude sensitivities are 218, 224 and 191 RIU^{-1} for gold layer thickness 30, 40 and 50 nm reciprocally. In figure 11 and 12 other factors like pitch, air hole diameters are unchanged.

4.3.4 Pitch variation

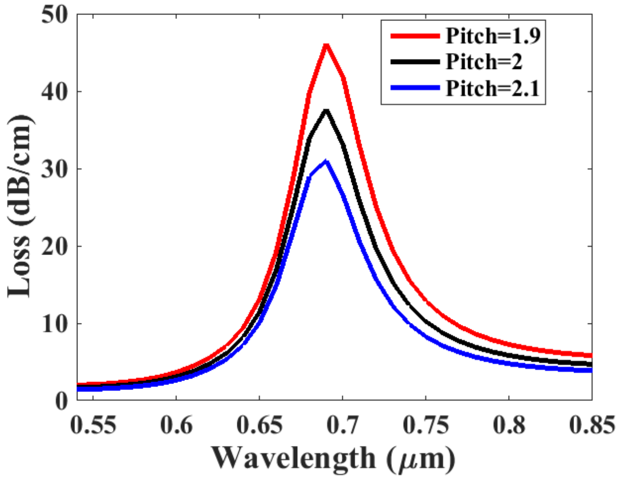

Figure 13: Loss spectrum with pitch variation.

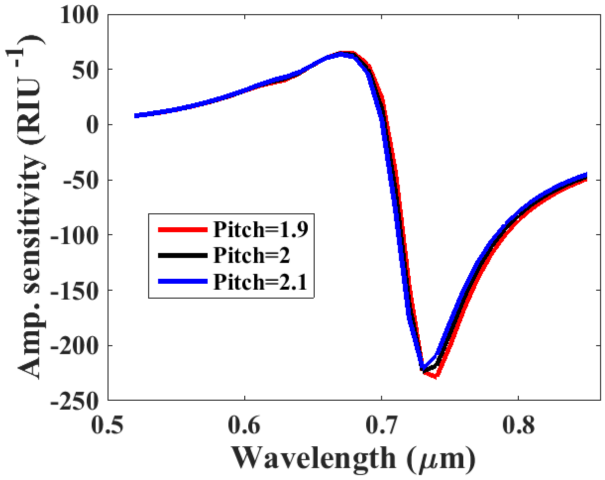

Figure 14: Amplitude sensitivity with pitch variation.

Figure 13. shows the loss spectrum for the change of pitch. Loss depths are 46, 37.7 and 31 dB/cm for the pitch value of 1.9, 2 and 2.1 μm in order. As a result of increase in pitch, effective RI distinction in core and cladding rises and so loss depth is decreased. Amplitude sensitivities are shown in Figure 14. for the variation of the pitch. For 1.9, 2 and 2.1 nm pitch, obtained amplitude sensitivities are 229, 224, 221 RIU^{-1} respectively. Figure 13 and 14 are for changed pitch but for unmoved air hole diameters, gold layer depth at RI 1.36.

4.3.5 Air hole diameter variation

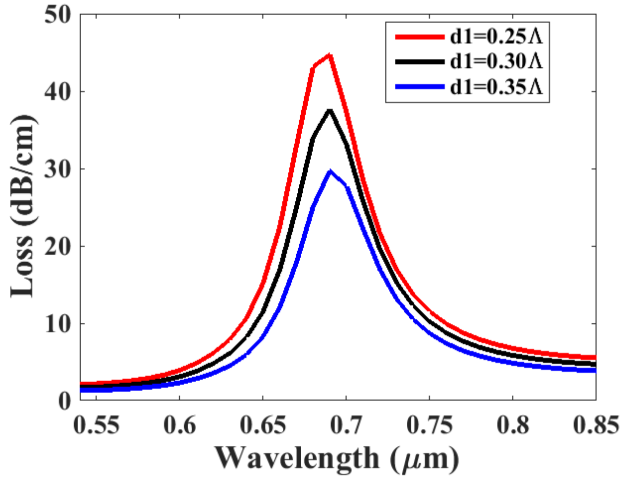

Figure 15: Loss spectrum with smaller air hole's diameter (d_1) variation.

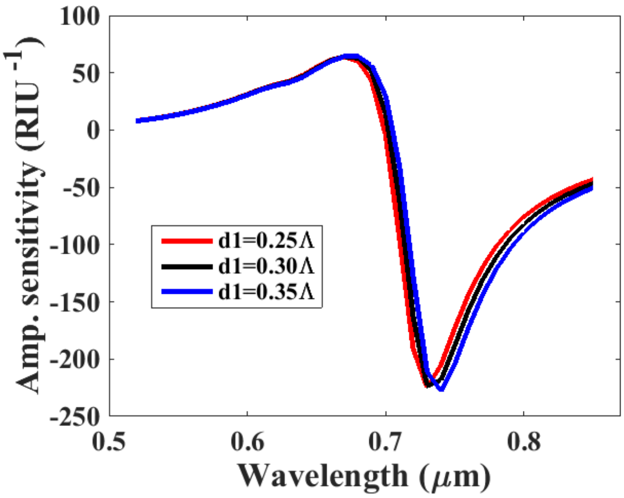

Figure 16: Amplitude sensitivity with smaller air hole's diameter (d_1) variation.

In Figure 15. the effect of the smaller air hole diameter (d_1) variation on the loss curve is explained. Loss depths are 45, 37.7, 30 dB/cm when the smaller air hole diameters are 0.25Λ, 0.3Λ and 0.35Λ respectively. Loss is decreased for the extended diameter of air hole. The changes of amplitude sensitivities with the alternation of smaller air hole diameters are depicted in Figure 16. When the diameters are 0.25Λ, 0.3Λ and 0.35Λ correspondingly, the amplitude sensitivities are 225, 224 and 228 RIU^{-1}. Figure 15, 16 are presented for similar value of pitch, d (bigger diameter), gold coating as optimum.

4.3.6 Linear Fitting

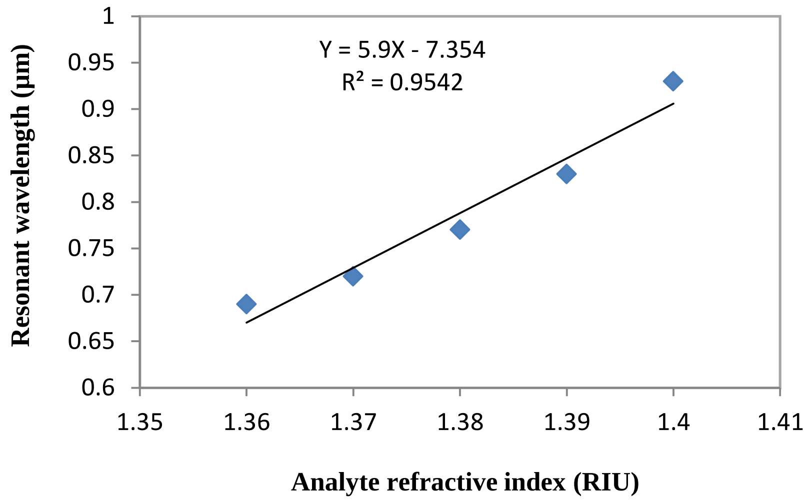

Figure 17: Linear fitting for t_g= 40 nm in the x-polarized mode

Figure 17. demonstrates resonated wavelength vs analyte refractive index graph. Their relation is linear fitted at 40 nm depth of gold layer. Average sensitivity is symbolized by linear fit curve's slope. In figure 17, linear fitting is described by the solid line and the resonant wavelengths are symbolized with the square marker. The value of R^2 embodies the resonant wavelength and analyte RI's connection. Linearity is desirable for the average sensitivity and resolution because it makes the detection process easier. The fitted line of figure 17 shows good linarity. Our offered design can be fabricated using chemical vapour deposition (CVD) method or atomic layer deposition (ALD) method. These methods are efficient for putting even gold coat on the rounded surface [6].

Table 1. Performance of the SPR sensor varying analyte refractive index

Analyte RI	Analyte RI difference	Peak Loss (dB/cm)	Resonance peak wavelength (nm)	Resonance peak shift (nm)	Wavelength Sensitivity (nm/RIU)	Wavelength Resolution (RIU)	Amplitude Sensitivity (RIU-1)	Amplitude Resolution (RIU)
1.36	0.01	37.7	690	30	3000	3.33×10^{-5}	224	4.46×10^{-5}
1.37	0.01	51.5	720	50	5000	2×10^{-5}	343	2.92×10^{-5}
1.38	0.01	76	770	60	6000	1.67×10^{-5}	560	1.79×10^{-5}
1.39	0.01	121	830	100	10000	1×10^{-5}	997	1×10^{-5}
1.40	0.01	218	930	N/A	N/A	N/A	N/A	N/A

Table 2. The proposed sensor versus existing sensors

References	Wavelength Sensitivity (nm/RIU)	Wavelength Resolution (RIU)	Amplitude Sensitivity (RIU^{-1})	Amplitude Resolution (RIU)
[2]	3700	2.7×10^{-5}	216	4.6×10^{-5}
[19]	2000	5×10^{-5}	80	12×10^{-5}
[20]	3000	3.33×10^{-5}	418	2.4×10^{-5}
[23]	2000	5×10^{-6}	300	3.3×10^{-5}
[26]	9180	1.09×10^{-5}	1739.26	5.75×10^{-6}
[27]	6000	1.67×10^{-5}	508	1.97×10^{-5}
[28]	23000	4.35×10^{-6}	820	1.22×10^{-5}
[29]	4000	2.5×10^{-5}	478	2.1×10^{-5}
[30]	4000	2.5×10^{-5}	320	3.125×10^{-5}
[31]	8000	1.25×10^{-5}	1560	8.64×10^{-5}
[32]	4600	2×10^{-5}	425	2×10^{-5}
[33]	4750	2.1×10^{-5}	1555	6.43×10^{-6}
[35]	2000	5×10^{-5}	140	7.1×10^{-5}
Proposed spiral PCF based sensor	10000	1×10^{-5}	997	1×10^{-5}

Various PCF based SPR sensors are studied in literature review section. The sensors having different designs show different features value. Table 2. represents the comparison between the performance of the proposed sensor with existing sensors.

Chapter 5

Conclusion and Future Work

5.1 Conclusion

To conclude, it can be said that bio sensor is a vital element to sense biochemical or biological analyte. Besides, SPR is one of the popular and effective technique for finding the unknown analyte. In past decades, prism based SPR sensors were well-liked. Two sensing methods were developed, such as Otto-configuration and Kretschmann-configuration. They had mechanical and optical parts. For this reason, they were bulky and roust. On the other hand PCF based SPR sensors are small in size. It's light propagation mechanism can be controlled by fluctuating the parameters. Now a days PCF based SPR sensors are admired a lot. In these type of sensors different plasmonic materials used for sensing purpose. These are gold, silver, aluminum, copper etc. Among them gold does not suffer from oxidization problem. Gold is more stable than the others. Placing this material and analyte into the sensor plays an important role. Putting the plasmonic material externally involves with practical fabrication. Analyte flow at the outer surface also ease the detection process. The value of sensitivity defines how accurately a sensor can sense. Using wavelength interrogation method and amplitude interrogation method sensitivity of a sensor is measured. At recent times highly sensitive sensor with excellent resolution is very demandable. Sensors which show linear appearances with high sensitivity are more attractive.

A spiral PCF based SPR sensor is proposed in this work. This sensor offers high sensitivity and improved resolution. Here, gold is used as plasmonic material. Both analyte layer and gold film are positioned at exterior surface of the PCF. The prime reasons are to minimize the fabrication difficulty and to have more practical sensing. Performance parameters are also investigated in this paper. Proposed sensor shows maximum wavelength sensitivity 10,000 nm/RIU and amplitude sensitivity 997 RIU^{-1} using optimized sensor parameters. This proposed sensor has dynamic detection rang. It is studied that our proposed sensor can response at refractive index range from 1.36 to 1.39. Resolution of this PCF based SPR sensor is 1×10^{-5} RIU. This highly resolutioned biosensor can be used for biological and biochemical analytes detection. This proposed sensor shows admirable linear properties. It has practical simplicity, suitable linearity and excellent sensing qualities.

5.2 Future Work

1. Due to fabrication challenges, PCF based sensors have limited practical applications. Most of the investigations are performed theoretically. Simulation model is also greatly used. So, experimental research for using PCF sensors in real-world appliances can be a dynamic upcoming research.

2. For detecting large amount of biological and biochemical analytes, PCF based sensor which can sense numerous refractive indices can be examined in future.

3. As PCF-based sensors are mainly employed in lab-oriented researches, in future commercialization of the sensors can be improved.

4. For future progress it is possible to implement this design by adding alternative plasmonic material outside the PCF surface.

5. SPR sensing technologies for THz frequencies can be improved. Moreover, in future, new design with improved performance can be implemented.

References

[1] M. R. Momota and M. R. Hasan, "Hollow-core silver coated photonic crystal fiber plasmonic sensor," Optical Materials, vol. 76, pp. 287-294, Feb.2018.

[2] J. N. Dash and R. Jha, "On the performance of graphene-based D-shaped photonic crystal fibre biosensor using surface plasmon resonance," Plasmonics, vol. 10, no. 5, pp. 1123-1131, 2015.

[3] A. A. Rifat, R. Ahmed, A. K. Yetisen, H. Butt, A. Sabouri, G. A. Mahdiraji, S. H. Yun and F. M. Adikan, "Photonic crystal fiber based plasmonic sensors," Sensors and Actuators B: Chemical, vol. 243, pp. 311-325, May 2017.

[4] J. Homola and M. Piliarik, "Surface Plasmon Resonance (SPR) Sensors," In Surface plasmon resonance based sensors, pp. 45-67, 2006.

[5] R. K. Gangwar and V. K. Singh, "Highly sensitive surface plasmon resonance based D-shaped photonic crystal fiber refractive index sensor," Plasmonics, vol. 12, no. 5, pp. 1367-1372, 2017.

[6] M. R. Hasan, S. Akter, A. A. Rifat, S. Rana, K. Ahmed , R. Ahmed, H. Subbaraman and D. Abbott, "Spiral Photonic Crystal Fiber-Based Dual-Polarized Surface Plasmon Resonance Biosensor," IEEE Sensors Journal, Vol. 18, no. 1, pp. 133-140, Jan. 2018.

[7] A. A. Rifat, G. A. Mahdiraji, Y. M. Sua, Y. G. Shee, R. Ahmed, D. M. Chow and F. M. Adikan, "Surface plasmon resonance photonic crystal fiber biosensor: a practical sensing approach," IEEE Photonics Technology Letters, vol. 27, no. 15, pp. 1628-1631, Aug. 2015.

[8] M. R. Hasan, S. Akter, K. Ahmed and D. Abbott, "Plasmonic refractive index sensor employing niobium nanofilm on photonic crystal fiber," IEEE Photonics Technology Letters, vol. 30, no. 4, pp. 315-318, Feb. 2018.

[9] A. A. Rifat, M. R. Hasan, R. Ahmed and H. Butt, "Photonic crystal fiber-based plasmonic biosensor with external sensing approach," Journal of Nanophotonics, vol. 12, no. 1, pp. 012503, Jun. 2017.

[10] R.W. Wood; "On a remarkable case of uneven distribution of light in a diffraction grating spectrum", Philosophical Magazine, vol. 4, pp. 396-402, 1902.

[11] A. Otto., "Exicitation of nonradiative surface plasma waves in silver by method of frustrated total reflection", Zeitschrift Fur Physik, vol. 216, pp. 398-410, 1968.

[12] I. Pockrand, J. D. Swalen, J.G. Gordon and M. R. Philpott; "Surface-plasmon spectroscopy of organic monolayer assemblies, " Surface Science, vol. 74, pp. 237-244, 1978.

[13] J.G. Gordon and S. Ernst; "Surface-plasmons as a porbe of the electrochemical interface," Surface Science, vol. 101, pp. 499-506, 1980.

[14] B. Liedberg, I. Lundstrom and E. Stenberg; "Principles of biosensing with an extended coupling matrix and surface plasmon resonance," Sensors And Actuators B-Chemical, vol. 11, pp. 63-72, 1993.

[15] K.M. McPeak, S.V. Jayanti, S.J. Kress, S. Meyer, S. Iotti, A. Rossinelli et al, "Plasmonic films can easily be better: rules and recipes," ACS Photonics, vol. 2, pp. 326–333, 2015.

[16] D. Gao, C. Guan, Y. Wen, X. Zhong and L. Yuan, "Multi-hole fiber based surface plasmon resonance sensor operated at near-infrared wavelengths," Optics Communications, vol. 313, pp. 94-98, 2014.

[17] Y. Lu, X. Yang, M. Wang and J. Yao, "Surface plasmon resonance sensor based on hollow-core PCFs filled with silver nanowires," Electronics Letters, vol. 51, no. 21, pp. 1675-1677, Oct. 2015.

[18] S. I. Azzam, M. F. O. Hameed, R. E. A. Shehata, A. M. Heikal and S. S. Obayya, "Multichannel photonic crystal fiber surface plasmon resonance based sensor," Optical and Quantum Electronics, vol. 48, no. 2, pp. 142, Jan. 2016.

[19] J.N. Dash, R. Jha, "SPR biosensor based on polymer PCF coated with conducting metal Oxide," IEEE Photonics, vol. 26, pp. 595–598 2014.

[20] A.A. Rifat, G.A. Mahdiraji, D.M. Chow, Y.G. Shee, R. Ahmed, F.R.M. Adikan, "Photonic crystal fiber-based surface plasmon resonance sensor with selective analyte channels and graphene-silver deposited core," Sensors, vol. 15, pp. 11499–11510, 2015.

[21] Z. Fan, S. Li, Q. Liu, G. An, H. Chen, J. Li et al, "High sensitivity of refractive index sensor based on analyte-filled photonic crystal fiber with surface plasmon resonance," IEEE Photonics, vol. **7**, pp. 1–9, 2015.

[22] C. Liu, L. Yang, X. Lu, Q. Liu, F. Wang, J. Lv et al, "Mid-infrared surface plasmon resonance sensor based on photonic crystal fibers," Opt. Express, vol. 25, pp. 14227–14237, 2017.

[23] P. Bing, J. Yao, Y. Lu, Z. Li, "A surface-plasmon-resonance sensor based on photonic-crystal-fiber with large size microfluidic channels," Opt. Appl, vol. 42, pp. 493–501, 2012.

[24] J.N. Dash and R. Jha, "Graphene-based birefringent photonic crystal fiber sensor using surface plasmon resonance," IEEE Photonics Technology Letters, vol. 26, no. 11, pp. 1092-1095, June 2014.

[25] G. An, S. Li, H. Wang and X. Zhang, “Metal oxide-graphene-based quasi-D-shaped optical fiber plasmonic biosensor,” IEEE Photonics Journal, vol. 9, no. 4, pp. 1-9, Aug. 2017.

[26] D. Li, W. Zhang, H. Liu, J. Hu and G. Zhou, “High sensitivity refractive index sensor based on multicoating photonic crystal fiber with surface plasmon resonance at near-infrared wavelength,” IEEE Photonics Journal, vol. 9, no. 2, pp. 1-8, Apr.2017.

[27] W.L. Ng, A.A. Rifat, W.R. Wong, G. Mahdiraji, F.M. Adikan, “A novel diamond ring fiber-based surface plasmon resonance sensor,” Plasmonics, pp. 1–6, 2017.

[28] A. A. Rifat, G. A. Mahdiraji, Y. M. Sua, R. Ahmed, Y. G. Shee and F. M. Adikan, “Highly sensitive multi-core flat fiber surface plasmon resonance refractive index sensor,” Optics express, vol 24, no. 3, pp. 2485-2495, Feb. 2016.

[29] A. A. Rifat, M. R. Hasan, R. Ahmed and H. Butt, “Photonic crystal fiber-based plasmonic biosensor with external sensing approach,” Journal of Nanophotonics, vol. 12, no. 1, pp. 012503, Jun. 2017.

[30] A. A. Rifat, G. A. Mahdiraji, Y. M. Sua, Y. G. Shee, R. Ahmed, D. M. Chow and F. M. Adikan, “Surface plasmon resonance photonic crystal fiber biosensor: a practical sensing approach,” IEEE Photonics Technology Letters, vol. 27, no.15, pp. 1628-1631, Aug. 2015.

[31] M. R. Hasan, S. Akter, K. Ahmed and D. Abbott, “Plasmonic refractive index sensor employing niobium nanofilm on photonic crystal fiber,” IEEE Photonics Technology Letters, vol. 30, no. 4, pp. 315-318, Feb. 2018.

[32] R. Otupiri, E.K. Akowuah, S. Haxha, “Multi-channel SPR biosensor based on PCF for multi-analyte sensing applications,” Opt. Express, vol. 23, pp. 15716–15727, 2015.

[33] M.F.O. Hameed, Y.K. Alrayk, A.A. Shaalan, W.S. El Deeb, S.S. Obayya, “Design of highly sensitive multichannel bimetallic photonic crystal fiber biosensor,” J. Nanophotonics, vol. 10, pp. 046016–04601, 2016.

[34] T. Huang, “Highly sensitive SPR sensor based on D-shaped photonic crystal fiber coated with indium tin oxide at near-infrared wavelength,” Plasmonics vol. 12, pp. 583–588, 2017.

[35] A.A. Rifat, G.A. Mahdiraji, R. Ahmed, D.M. Chow, Y. Sua, Y. Shee et al, “Copper-graphene based photonic crystal fiber plasmonic biosensor,” IEEE Photonics J., vol. 8, pp. 1–8, 2016.

[36] S.I. Azzam, M.F.O. Hameed, R.E.A. Shehata, A. Heikal, S.S. Obayya, “Multichannel photonic crystal fiber surface plasmon resonance based sensor,” Opt. Quant. Electron, vol. 48, pp. 142, 2016.

[37] Warren J. Smith, Modern Optical Engineering, Prentice Hall, 5th edition, pp. 20-26, 2005.

[38] Dinesh Kumar Prajapati, Ramesh Bharti, "Dispersion analysis of a Hybrid Photonic Crystal Fiber," International Journal of Recent Research and Review, vol. 7, no. 2, pp. 118-122, Jun. 2014.

[39] Md. Selim Habib, Md. Samiul Habib, S.M.A. Razzak, "Study on Dual-Concentric-Core Dispersion Compensating Photonic Crystal Fiber," International Journal of Engineering and Technology, vol. 4, no. 1, pp. 377-383, Sep. 2012.

[40] R. Buczynski, "Photonic Crystal Fibers," International School of Semiconducting Compounds, vol. 106, no. 2, pp. 141-168, Jun. 2004.

[41] Philip Russell, "Photonic Crystal Fibers: A Historical Account," IEEE Leos Newsletter, vol. 21, no. 5, pp. 11-15, Oct. 2007.

[42] J. Limpert, O. Schmidt, J. Rothhardt, F. Roser, T. Schreiber, and A. Tunnermann, "Extended single-mode photonic crystal fiber lasers," Optic Express, vol. 14, no. 7, pp. 2715-2720, Apr.2006.

[43] Jonathan C. Knight, "Photonic crystal fibres," Nature international weekly journal of science, vol. 424, pp. 847-851, Aug. 2003.

[44] E. Yablonovitch, "Photonic band-gap structures," Journal of Optical Society, vol. 10, no. 2, pp. 283-295, Feb. 1993.

[45] Ming-Yang Chen, "Polarization and leakage properties of large mode-area microstructured-core optical fibers," Optics Express, vol. 15, no. 19, pp. 12498-12507, Sep. 2007.

[46] M.I. Hasan, M. Selim Habib, M. Samiul Habib, S.M. Abdur Razzak, "Highly nonlinear and highly birefringent dispersion compensating photonic crystal fiber," Optical Fiber Technology, vol. 20, no. 1, pp. 32-38, Jan. 2014.

[47] P. K. Maharana, P. Padhy and R. Jha; "On the field enhancement and performance of an ultrastable SPR biosensor based on grapheme," IEEE Photonics Technoogy. Lett., vol. 25, no. 22, pp. 2156-2159, 2013.

[48] K. Sharma, R. Jha and B. D. Gupta, "Fiber-optic sensors based on surface plasmon resonance: a comprehensive review," IEEE Sensors Journal, vol. 7, no. 8, pp. 1118-1129, Aug. 2007.

[49] B. D. Gupta and R. K. Verma, "Surface Plasmon Resonance-Based Fiber Optic Sensors: Principle, Probe Designs, and Some Applications," Journal of Sensors, vol. 2009, Jun. 2009.

[50] E. K. Akowuah, T. Gorman, and S. Haxha*, "Design and optimization of a novel surface plasmon resonance biosensor based on Otto configuration," Journal of Sensors, vol. 17, no. 26, pp. 23511-23521, Dec.2009.

[51] Hyuk Rok Gwon and Seong Hyuk Lee. "Spectral and Angular Responses of Surface Plasmon Resonance Based on the Kretschmann Prism Configuration," Materials Transactions, vol. 51, no. 6, pp. 1150-1155, Apr.2010.

[52] Tomas Rindzevicius, Yury Alaverdyan, Andreas Dahlin, Fredrik Ho1o1k, Duncan S. Sutherland, and Mikael Ka1ll, "Plasmonic Sensing Characteristics of Single Nanometric Holes," Nano Letters, vol. 5, no. 11, pp. 2335-2339, Oct. 2005.

[53] Bertrand Gauvreau, Alireza Hassani, Majid Fassi Fehri, Andrei Kabashin, Maksim Skorobogatiy, "Photonic bandgap fiber-based Surface Plasmon Resonance sensors," Optic Express, vol. 15, no. 18, pp. 11413-11426, Sep. 2007.

[54] Hikmat N. Daghestani1 and Billy W. Day2*, "Theory and Applications of Surface Plasmon Resonance, Resonant Mirror, Resonant Waveguide Grating, and Dual Polarization Interferometry Biosensors," Sensors, vol. 10, pp. 9630-9646, Nov. 2010.

[55] Brian H. Dennis, Weiya Jin, George S. Dulikravich, Jovo Jaric, "Application of the Finite Element Method to Inverse Problems in Solid Mechanics," International Journal of Structural Changes in Solids, vol. 3, no. 2, pp. 11-21, Jun. 2011.

[56] Ray W. Clough, "Original formulation of the finite element method," Elsevier, vol. 7, pp. 89-101, 1990.

[57] Jeav-Pierre Berenger, "A Perfectly Matched Layer for the Absorption of Electromagnetic Waves," Journal of computational physics, vol. 114, pp. 185-200, 1994.

[58] M.C Amann and B. Stegmuller, "Calculation of the effective refractive index step for the metal-cladded-ridge waveguide laser," Journal of computational physics, vol. 20, pp. 1483-1486, Nov. 1981.

[59] Md. Selim Habib, Md. Samiul Habib, and S.M.A. Razzak, "Study on dual-concentric-core dispersion compensating photonic crystal fiber," International J. of Eng. and Technol., vol. 1, no. 4, pp. 377-383, 2012.

[60] Md. Selim Habib, Md. Samiul Habib, S.M. Abdur Razzak, Yoshinori Namihira, M.A. Hossain, and M.A. Goffar Khan, "Broadband dispersion compensation of conventional single mode fibers using microstructure optical fibers," Optik, vol. 124, no. 19, pp. 3851-3855, Oct. 2013.